Performance analysis of OFDM modulation on indoor PLC channels in the frequency band up to 210 MHz

Juan José Sánchez-Martínez[1], José Antonio Cortés, Luis Díez, Francisco Javier Cañete
Departamento de Ingeniería de Comunicaciones
E.T.S.I. de Telecomunicación, University of Málaga, Spain
Email: [1]jjsm@ic.uma.es

Luis M.Torres
Design of Systems on Silicon (DS2)
C/Charles Robert Darwin 2, Parc Tecnológic,
46980 Paterna, Valencia, Spain.
Email: luismanuel.torres@ds2.es

***Abstract*—This paper analyses the performance of Orthogonal Frequency-Division Multiplexing (OFDM) systems on indoor power line. The studied frequency band extends up to 210MHz, as specified in the upcoming International Telecommunication Union (ITU) G.hn standard for wired home networks. Four frequency bands have been considered, from 1MHz up to 30MHz, from 30MHz up to 86MHz, from 1MHz up to 86MHz and from 110MHz up to 210MHz. Conventional OFDM modulation with rectangular pulses and OFDM with pulse-shaping at the transmitter and non-rectangular window at the receiver are assessed. Bit-rates attained with both schemes are evaluated as a function of the number of carriers and the cyclic prefix length. Presented results can be used to select the most appropriate system parameters for each frequency band.**

I. Introduction

Nowadays, power lines have become an attractive solution to provide the broadband data connections required by the high-speed home media applications and triple play services in small offices and homes. Up to now, the lack of an international technical standard has been a barrier to the expansion of Power Line Communications (PLC) technology. However, the approved ITU-T G.hn recommendation for in-home networking is expected to solve this situation. The new standard promises high quality multimedia over power, coaxial, phone and other home wiring.

Indoor power line channels are frequency and time selective, with remarkable disparity even among different locations in a specific site. The frequency selective characteristics of indoor power line channels in the frequency band up to 30 MHz have been reported in [1],[2],[3],[4]. Recent studies have extended the analysis up to 100MHz [5], [6]. Time variations have a twofold nature: long-term changes caused by the connection and disconnection of electrical appliances and periodic short-term changes, synchronous with the mains, due to the time-variant behavior of the impedance and the noise emitted by the electrical devices [7]. Regarding the noise, it is composed of the following terms: coloured background noise, impulsive components and narrowband interferences [8].

OFDM is a suitable technique to cope with the aforementioned impairments. Its performance is essentially determined by the number of carriers and the cyclic prefix length. An improvement can be achieved considering pulse-shaping at the transmmiter and windowing at the receiver. Previous works [9],[10],[11] have dealt with this optimization problem but, to the author's knowledge, this is the first study in which the analysis is accomplished in the frequency band up to 210 MHz. In this context, we make two main contributions:

- We evaluate the performance of OFDM in the band up to 210MHz for the first time. The whole band is split up into four sub-bands that are assessed separately.
- We determine the system parameters (number of carriers, the guard interval length, and the transmiter and receiver pulses length) that maximize the performance in each frequency band.

The organization of the paper is as follows. Firstly, the channel model and the employed OFDM systems are described in section II. Performance analysis is presented in section III. Finally, main conclusions are drawn in section IV.

II. System model

A. Channel model

The channel model considered in this work consists of a linear and time-invariant (LTI) filter and a stationary Gaussian colored noise. Hence, the periodic time variation of the channel is disregarded. However, the following reasons make this simplification not to limit the validity of the results presented in this paper. The first one is that the delay spread of PLC channels, which strongly determines the cyclic prefix length, is essentially time invariant [12]. Therefore, the most appropriate value for the cyclic prefix length can be obtained from an LTI channel response measured at any time instant within the mains cycle. The second reason is that the maximum number of carriers considered in this work is limited to 4096, which is in the order of the values employed by current commercial systems. As shown in [13], the distortion caused by the channel time variation for this number of carriers is negligible.

Estimated channel responses and noise power spectral densities (PSD) used in this work have been drawn from a set of more than 160 channels measured by DS2 [14] in more than 20 different sites. However, for the sake of simplicity, only a subset of them have been used in the analysis. These estimated channel responses and noise PSD are the time-averaged component of the time-varying channel responses and the instantaneous noise PSD which characterize indoor power-line channels [7].

The employed channel responses have been selected according to their delay spread and their average amplitude response, so that they represent the whole set. To this end, the cumulative distribution function (CDF) of the delay spread has been computed. Two channels responses of each quartile have been taken: the ones with the lowest and the largest average attenuation. This process is accomplished for each of the four bands considered in the analysis: 1-30 MHz, 30-86 MHz, 1-86 MHz and 110-210 MHz. The selection of the noise PSD is performed according to noise power and the peakedness of the PSD in the considered frequency band. The peakedness (PK) of the PSD provides an indication of the amount of narrowband components (caused by periodic impulsive noise or interferences) of the PSD.

Table I shows the number of channels and noise PSDs employed in each band.

TABLE I
NUMBER OF CHANNELS USED IN SIMULATIONS

Frequency band (MHz)	1-30	30-86	1-86	110-210
Number of channel responses	8	8	8	8
Number of noise PSD	6	6	5	6
Total number of channel	48	48	40	48

B. OFDM system model

Two OFDM systems are considered in this work. The first one, referred to as conventional OFDM, employs rectangular pulses both at the transmitter and at the receiver. The second one, named as pulse-shaped and windowing OFDM, is characterized by using non-rectangular pulses neither at the transmitter nor at the receiver.

The main problem of the conventional OFDM is its reduced spectral containment due to the use of rectangular pulses. The sinc-shaped spectrum of these pulses, with a low decay of the side lobes, has a direct implication both in the trasmitter side, with the constraint of a PSD mask, and in the receiver side, when distortion appears in real systems. For instance: when the guard interval is not enough to compensate for the effect of channel time dispersion, or due to non-pefect synchronization, or due to the doppler spread created by the time-varying channel. Both drawbacks can be minimized with reduced implementation complexity by means of the so-called pulse-shaping and windowing techniques. Pulse-shaping techique was proposed, before the invention of the equalization by means of the cyclic prefix, as a mean for reducing the intercarrier interference (ICI) in time dispersive channels [15]. By means of a time-domain pulse shaping of the OFDM symbols, with a proper roll-off, it is possible to generate deep frequency notches. By doing so, carriers close to the PSD mask limits, which should be turned off if rectangular-pulses were used, can now be employed. Windowing technique was proposed as a way to reduce the effect of RF interferences in VDSL [16]. The use of a non-rectangular window at the receiver reduces the effect of the colored noise and of the intercarrier interference.

In a conventional OFDM system with N carriers, the last cp samples of the Inverse Discrete Fourier Transform (IDFT) are prepended to the beginning of the N samples to conform the cyclic prefix. In the pulse-shaped and windowed OFDM system three different parts are now added to the N output samples of the IDFT. The N samples are extended at both ends, $\alpha + \beta + GI$ samples at its beginning and α samples at its ending. The first and last α samples are shaped at the transmitter by multiplying by a non-rectangular window. In this work, a raised-cosine window is employed. In order to minimize the symbol rate loss the pulse-shaped symbols are partially overlapped as shown in Fig. 1.

Fig. 1. Structure of the pulse-shaped and windowed OFDM symbols.

At the receiver, the α samples at the beginning and the end of the symbol are discarded. The GI samples used to absorb the channel distortion are also discarded. The resulting $\beta + N$ samples are windowed and time aliased [16]. The complex values transmitted in each carrier are then obtained by performing an N-point DFT of the resulting signal. Fig. 2 shows noise power at the output of the DFT for different values of β. The benefit of using a non-rectangular window at the receiver can be clearly observed even for small values of β. This effect is more prominent in frequencies close to the FM radio band.

In both OFDM systems the transmitted signal complies with the PSD mask established in the G.9960 Recommendation for operation on power lines, shown in Fig. 3. Amateur radio bands are not considered.

In these circumstances, the bit-rate achieved in the m-th channel by the conventional OFDM system (denoted with superindex c) when employing N carriers and cp samples of cyclic prefix can then be obtained according to

$$R_m^c(N, cp) = \frac{f_s}{N + cp} \sum_{k=0}^{N-1} b_m^c(k), \tag{1}$$

where f_s is the sampling frequency and $b_m^c(k)$ is the number of bits per symbol transmitted in the k-th carrier. For the sake of clarity, the dependence of the number of bits per symbol with N and cp is obviated in the notation. Provided that both the noise and the distortion caused by the channel have a Gaussian distribution, $b_m^c(k)$ can be obtained according to

$$b_m^c(k) = \left\lfloor \log_2 \left(1 + \frac{SNDR_m^c(k)}{\Gamma} \right) \right\rfloor, \tag{2}$$

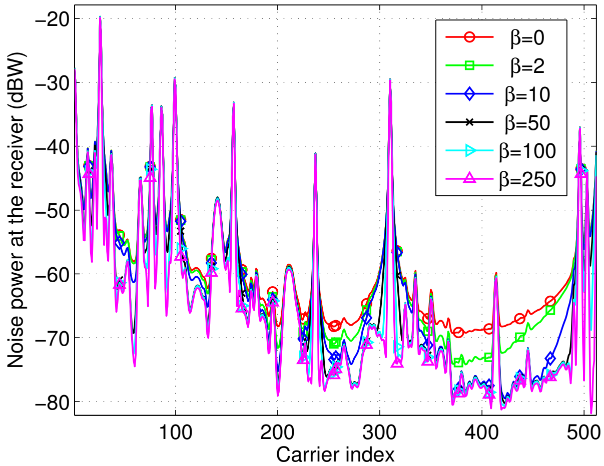

Fig. 2. Noise power at the outputs of the DFT performed at the receiver in the frequency band 1-86 MHz.

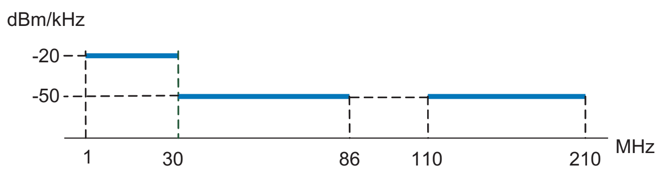

Fig. 3. Transmission PSD mask in the frequency band from 1 MHz to 210 MHz.

where $SNDR_m^c$ is the signal to noise and distortion ratio and Γ is the so-called *SNR gap*, which models the signal to noise ratio (SNR) penalty experienced because of the use of a discrete constellation [17]. For square QAM constellations it can be approximated by [18]

$$\Gamma = -\frac{1}{1.6} \ln \left(\frac{\text{BER}}{0.2} \right), \tag{3}$$

where BER is the bit error rate.

Similarly, the bit-rate achieved by the pulse-shaped and windowed OFDM system in the m-th channel (denoted with superindex pw) is given by

$$R_m^{pw}(N, \alpha, \beta, GI) = \frac{f_s}{N + \alpha + \beta + GI} \sum_{k=0}^{N-1} b_m^{pw}(k), \tag{4}$$

where $b_m^{pw}(k)$ is the number of bits per symbol transmitted in the k-th carrier.

The values of signal to noise and distortion ratio are calculated in two steps. Firstly, all masked carriers (carriers allowed to transmit) are used to transmit and the SNDR is computed at the receiver. Then, the bit-loading is accomplished by assigning to each carrier the nearest constellation that results from rounding the numbers of bits calculated to the nearest lower integer. If during this process some carrier is switched off, the SNDR is recalculated.

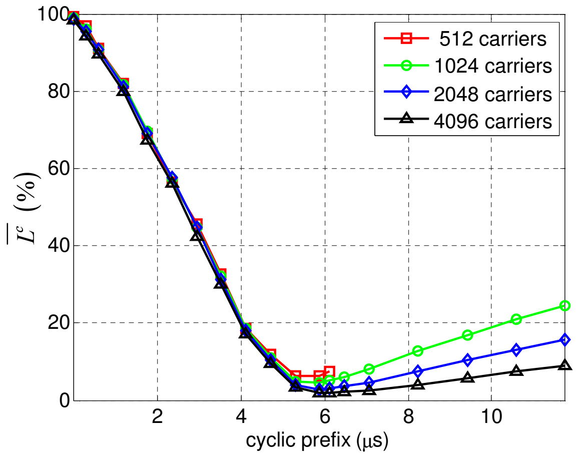

Fig. 4. Averaged bit-rate loss in the 1-86 MHz band as a function of the number of carriers and cyclic prefix length.

III. Performance Analysis

This section shows the performance evaluation results of both OFDM systems. Simulations have been accomplished using Binary PSK and square QAM constellations with a maximum of 14 bits per symbol and a BER constraint of 10^{-3}. Nowadays, a bit cap of 12 bits is employed in commercial devices, but from a theoretical point of view and to evaluate the performance of OFDM this limit has been extended up to 14 bits.

A. Conventional OFDM system

Let's consider an OFDM system with N carriers. The bit-rate loss caused by the use of a non-optimum cyclic prefix in the m-th channel is given by

$$L_m^c(N, cp) = 1 - \frac{R_m^c(N, cp)}{\max\limits_{cp}\{R_m^c(N, cp)\}}, \tag{5}$$

and the averaged bit-rate loss over the M considered channels is calculated from

$$\overline{L^c}(N, cp) = \frac{1}{M} \sum_{m=1}^{M} L_m^c(N, cp). \tag{6}$$

This parameter is now used as a performance indicator to determine the most appropriate values for the number of carriers and cyclic prefix length. Fig. 4 depicts the values of (6) for the 1-86 MHz band expressed as a percentage. The curves for the other bands exhibit the same tendency. For small cyclic prefix values the average bit-rate loss diminishes as the cyclic prefix increases. However, once the reduction of the distortion does not compensate for the symbol rate loss, increasing the cyclic prefix length also increases the average bit-rate loss. It should be noticed that the maximum cyclic prefix length when using $N = 512$ is limited to about 6 μs, which correspond to the case where $cp = N$.

Table II shows the values of the cyclic prefix that minimize (6), which from now on will be referred to as the optimum ones.

TABLE II
OPTIMUM CYCLIC PREFIX LENGTHS (μs) AS FUNCTION OF THE NUMBER OF CARRIERS

	Number of carriers			
Frequency band (MHz)	512	1024	2048	4096
1-30	6.03	6.03	6.03	6.89
30-86	2.68	3.12	3.12	3.12
1-86	5.88	5.88	5.88	5.88
110-210	2.25	2.50	2.50	2.50

Results shown in Table II indicate that the frequency bands from 1 MHz to 30 MHz and from 1 MHz to 86 MHz require longer cyclic prefix lengths than the remaining ones. This is consistent with the fact that the frequency selectivity of PLC channels is much greater in the frequency band below 30MHz. It is also interesting to notice that the optimum cyclic prefix lengths in the frequency band from 1 MHz to 86 MHz are smaller than in the band from 1 MHz to 30 MHz. This is due to the characteristics of the PSD mask employed at the transmitter, which has an abrupt transition with a gap of 30 dB at 30 MHz. This makes the carriers below 30 MHz to produce an enormous ICI in the carriers above 30 MHz. The reduction of this ICI term with the cyclic prefix is so small that it does not compensate for the reduction of the symbol rate it causes.

Although optimum cyclic prefix values for each frequency band have been previously determined, it is interesting to show the cyclic prefix value that maximize the bit-rate in each channel. Fig. 5 shows the CDF of these cyclic prefixes for both the 1-30 MHz and the 110-210 MHz bands. It can be seen that dispersion of the optimum values are smaller in the frequency band from 110 MHz to 210 MHz, which indicates that channels in this band are more homogeneous than in the low frequency band.

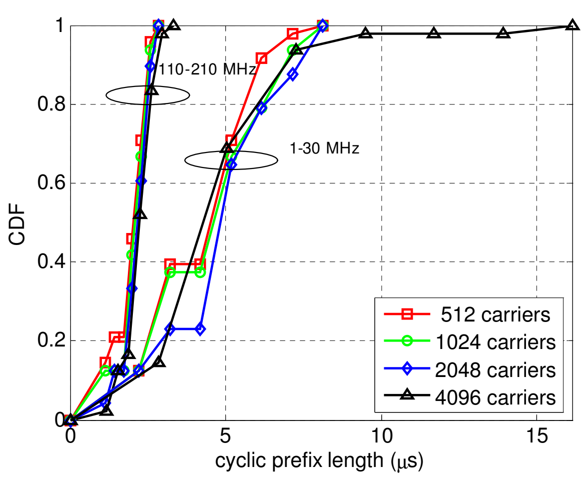

Fig. 5. CDF of the optimum cyclic prefix in each channel for the 1-30 and 110-210 frequency bands.

Using the cyclic prefix values given in Table II cause each channel to experience a certain bit-rate loss, since these values are optimum on average. Table III summarizes the maximum bit-rate loss experienced in 90% of the channels when using values listed in Table II. Similarly, Table IV contains the maximum bit-rate achieved in 90% of the channels. As seen, increasing the number of carriers produces significant performance improvements.

TABLE III
MAXIMUM BIT-RATE LOSS IN 90% OF THE CHANNELS USING THE CYCLIC PREFIX VALUES GIVEN IN TABLE II

	Number of carriers			
Frequency band (MHz)	512	1024	2048	4096
1-30	13%	8%	5%	3%
30-86	7.5%	5%	3.5%	2%
1-86	17%	12%	7%	4%
110-210	8%	5%	2%	1%

TABLE IV
MAXIMUM BIT-RATE (MBIT/S) IN 90% OF THE CHANNELS USING THE CYCLIC PREFIXES OF TABLE II.

	Number of carriers			
Frequency band (MHz)	512	1024	2048	4096
1-30	260	300	320	330
30-86	460	540	550	600
1-86	500	680	810	900
110-210	800	940	1050	1110

B. *Pulsed-shaped and windowed OFDM system*

Following a similar procedure, the averaged bit-rate loss over the M considered channels in each band is given by

$$\overline{L^{pw}}(N,\alpha,\beta,GI) = \frac{1}{M}\sum_{m=1}^{M} L_m^{pw}(N,\alpha,\beta,GI), \qquad (7)$$

where $L_m^{pw}(N,\alpha,\beta,GI)$ is the bit-rate loss caused by the use of non-optimum values of α, β and GI in the m-th channel and is given by

$$L_m^{pw}(N,\alpha,\beta,GI) = 1 - \frac{R_m^{pw}(N,\alpha,\beta,GI)}{\max\limits_{\alpha,\beta,GI}\{R_m^{pw}(N,\alpha,\beta,GI)\}}. \qquad (8)$$

For a given value of N expression (8) depends on three variables. The resulting graph can be drawn setting the value of one of them and varying the other two on a three-dimensional graphic as depicted in Fig. 6. The values of GI, α and β that minimize 7 are listed in Table V.

Fig. 7, 8, 9 and 10 represent the CDF of the bit-rate gain obtained with the pulse-shaped and windowed OFDM system with respect to the conventional one. The optimum values listed in Table V are used in the pulse-shaped and windowed OFDM system and the ones given in Table II in the conventional OFDM system. As seen, similar gains are obtained in all the frequency bands. As expected, in all cases the bit-rate gains decrease as the number of carriers is increased. This is not a surprising result, since the conventional OFDM is a channel capacity achieving strategy for $N \to \infty$.

TABLE V
OPTIMUM VALUES OF GI, α AND β IN (μs) AS FUNCTION OF THE NUMBER OF CARRIERS IN EACH FREQUENCY BAND

	Frequency band (MHz)											
	1-30			30-86			1-86			110-210		
Number of carriers	GI	α	β	GI	α	β	GI	α	β	GI	α	β
512	4.31	0.07	0.69	1.78	0.04	1.36	2.47	0.59	1.18	2	0.02	0.5
1024	4.31	0.07	1.72	2.23	0.04	1.36	3.29	0.94	0.94	1.75	0.02	0.86
2048	4.31	0.07	1.72	2.23	0.04	1.36	3.53	0.94	1.18	1.75	0.02	0.86
4096	4.31	0.34	1.72	2.23	0.04	1.36	3.53	1.17	1.18	1.75	0.02	1

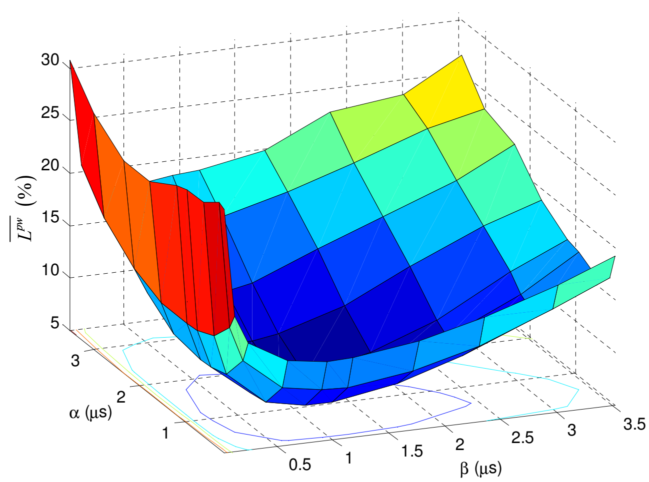

Fig. 6. Averaged bit-rate loss as a percentage varying α and β for the 1-86 MHz frequency band with 1024 sub-carriers and GI=3.29 μs.

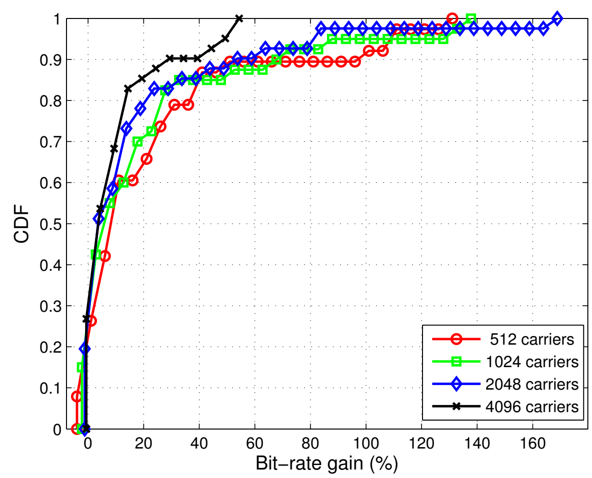

Fig. 8. CDF of the bit-rate gain obtained with the pulse-shaped and windowed OFDM system with respect to the conventional one in the 30-86 MHz frequency band.

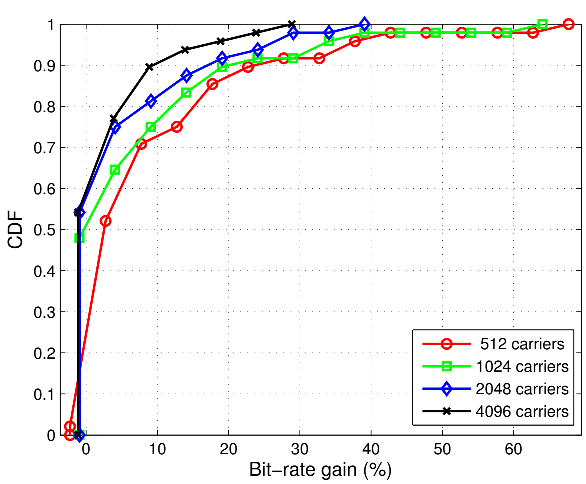

Fig. 7. CDF of the bit-rate gain obtained with the pulse-shaped and windowed OFDM system with respect to the conventional one in the 1-30 MHz frequency band.

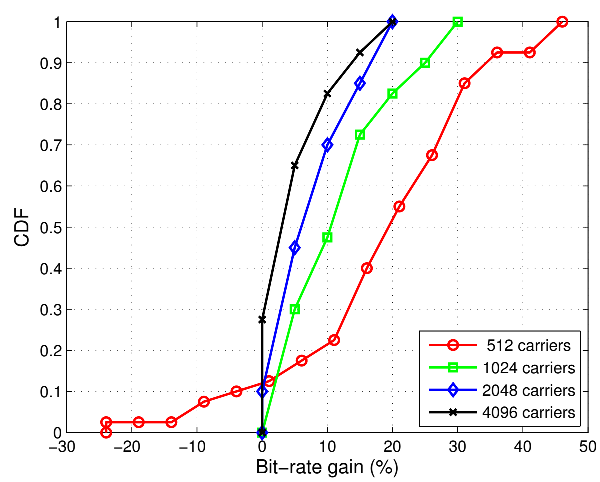

Fig. 9. CDF of the bit-rate gain obtained with the pulse-shaped and windowed OFDM system with respect to the conventional one in the 1-86 MHz frequency band.

IV. CONCLUSION

This paper has analyzed the performance of OFDM systems on indoor power line channels in the frequency band up to 210 MHz, as specified in the upcoming ITU G.hn standard. Conventional OFDM modulation with rectangular pulses and OFDM with pulse-shaping at the transmitter and non-rectangular window at the receiver are considered. The

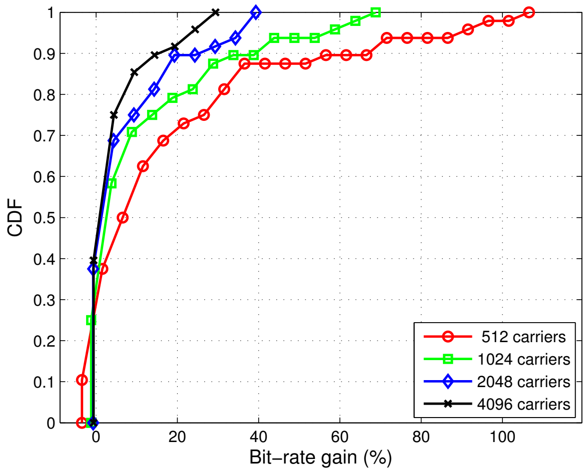

Fig. 10. CDF of the bit-rate gain obtained with the pulse-shaped and windowed OFDM system with respect to the conventional one in the 110-210 MHz frequency band.

performed study has been carried out using a set of more than 160 measured channels in four frequency bands: 1-30 MHz, 30-86 MHz, 1-86 MHz and 110-210 MHz. Optimum values of the system parameters have been provided, and the bit-rate gains achieved by the use of the OFDM system with pulse-shaping and windowing have been given.

References

[1] H. Philipps, "Performance measurements of power-line channels at high frequencies," in *Proceedings of the International Symposium on Power Line Communications and its Applications (ISPLC)*, 1998, pp. 229–237.

[2] V. Degardin, M. Lienard, A. Zeddam, F. Gauthier, and P. Degauque, "Classification and characterization of impulsive noise on indoor power line used for data communications," *IEEE Transactions on Consumer Electronics*, vol. 48, no. 4, pp. 913–918, November 2002.

[3] F. J. Cañete, L. Díez, J. A. Cortés, and J. T. Entrambasaguas, "Broadband modelling of indoor power-line channels," *IEEE Transactions on Consumer Electronics*, pp. 175–183, Feb 2002.

[4] T. Esmailian, F. R. Kschischang, and P. G. Gulak, "In-building power lines as high-speed communication channels: channel characterization and a test channel ensemble," *International Journal of Communications*, vol. 16, pp. 381–400, June 2003.

[5] M.Tlich, A. Zeddam, F. Moulin, and F. Gauthier, "Indoor Power-Line Communications Channel Characterization up to 100 MHz-Part I: One-Parameter Deterministic Model," *IEEE Transaction on power delivery*, vol. 23, no. 3, pp. 1392–1401, July 2008.

[6] ——, "Indoor Power-Line Communications Channel Characterization up to 100 MHz-Part II: Time-Frequency Analysis," *IEEE Transactions on power Delivery*, vol. 23, no. 3, pp. 1402–1408, July 2008.

[7] F. J. Cañete, J. A. Cortés, L. Díez, and J. T. Entrambasaguas, "Analysis of the cyclic short-term variation of indoor power line channels," *IEEE Journal on Selected Areas on Communications*, vol. 24, no. 7, pp. 1327–1338, July 2006.

[8] M. Zimmermann and K. Dostert, "Analysis and modeling of impulsive noise in broad-band powerline communications," *IEEE Transactions on Electromagnetic Compatibility*, vol. 44, no. 1, pp. 249–258, February 2002.

[9] J. A. Cortés, L. Díez, F. J. Cañete, and J. T. Entrambasaguas, "System parameters effect on DMT-based broadband indoor power line communications," in *International Symposium on Power-Line Communications and its Applications (ISPLC)*, 2002, pp. 48–52.

[10] K. H. Afkhamie, H. Latchman, L. Yongel, and T. D. R. Newman, "Joint Optimization of Transmit Pulse Shaping, Guard Interval length, and receiver side narrow-band interference mitigation in the HomePlugAV OFDM system," in *IEEE Workshop on Signal Processing Advances in Wireless Communications*, June 2005, pp. 5–8.

[11] A. Tonello, S. D'Alessandro, and L. Lampe, "Bit, Tone and Cyclic Prefix Allocation in OFDM with Application to In-Home PLC," in *IEEE IFIP Wireless Days Conference*, November 2008, pp. 23–27.

[12] J. A. Cortés, F. J. Cañete, L. Díez, and J. T. Entrambasaguas, "Characterization of the cyclic short-time variation of indoor power-line channels response," in *Proceedings of the International Symposium on Power Line Communications and its Applications (ISPLC)*, 2005, pp. 326–330.

[13] J. A. Cortés, "Modulation and multiple access techniques for indoor broadband power-line communications," Ph.D. dissertation, ETSI de Telecomunicación, Universidad de Málaga, 2007.

[14] Design of Systems on Silicon (DS2). [Online]. Available: www.ds2.es.

[15] S. B. Weinstein and P. M. Ebert, "Data transmission by frequency-division multiplexing using de discrete fourier transform," *IEEE Transactions on Communications*, vol. 19, no. 5, pp. 628–634, Oct 1971.

[16] P. Spruyt, P. Reusens, and S. Braet, "Performance of improved DMT transceiver for VDSL," Tech. Report T1E1.4/96-104, ANSI, Colorado Springs, CO, Apr., Tech. Rep., 1996.

[17] E. Lee and D. Messerschmitt, *Digital Communication*. Kluwer Academic Publishers, 1994.

[18] S. T. Chung and A. J. Goldsmith, "Degrees of freedom in adaptive modulation: A unified view," *IEEE Transactions on Communications*, vol. 49, no. 9, pp. 1561–1571, September 2001.